Indonesian Geotechnical Journal, April 2022, Vol 1 (1). Page 41-57
DOI: https://doi.org/10.56144/igj.v1i1.7
E-ISSN 2829-7520
https://indonesian-geotechnical-journal.org/index.php/JGI/issue/archive

The Analysis of Pile-Pile Cap Behavior Under Static Loading Test Using Distributed Fiber Optic Sensor

Tanti Muliati[1,*], Paulus Pramono Rahardjo[1], Bondan Widi Anggoro[2], Ricky Setiawan[2]
[1] Civil Engineering Department, Parahyangan Catholic University, Bandung, Indonesia; rahardjo.paulus@gmail.com
[2] PT Geotechnical Engineering Consultant, Bandung, INDONESIA; bondananggoro9954@gmail.com; rickysetiawan.geo@gmail.com
*Correspondence: muliati.tanti@gmail.com

SUBMITTED 5 April 2022 **REVISED** 18 April 2022 **ACCEPTED** 20 April 2022

ABSTRACT Pile-Pile cap behavior was investigated in this study through the utilization of fiber optic sensors to continuously transmit information along the bored pile at a reading interval of 40 mm during each cycle of the static loading test. It is important to note that the fiber optic cables were installed on the two sides of the bored pile connected up to the pile cap to monitor the stress distribution beneath the pile cap while fiber optic sensors were installed under the pile cap. The ultimate axial bearing capacity expected to be achieved using the pile-pile cap configuration was 190 tons x 250% but failure occurred when the load used was increased to 190% of the design load. Therefore, the strain measurement obtained from the Distributed Fiber Optic Sensor Technology was analyzed to obtain information on the load transfer, pile shortening, mobilized unit skin friction, and mobilized end bearing at the pile-pile cap. The load portion carried out by pile cap was approximated at 6% to 23% from the actual top load applied. It was also discovered that the fiber optic sensors initially installed were able to record the strain caused to the soil by the load on the pile cap. The strain measurements on the soil made the zone of influence due to the loading of the foundation to reach two times the length of the pile while the biggest zone of influence lies at the end of the foundation. From recorded strain, show higher strain from one side compared to the other, this may indicate eccentricity of the load.

KEYWORDS Pile-pile cap system, Bored pile foundation, Fiber optic sensors, Static load test, Strain, BOTDA

1 INTRODUCTION

The allowable capacity in a foundation system can be determined by dividing the ultimate capacity by a certain safety factor. It is important to note that carrying capacity assumes all loads are carried only by the pile foundations in practice but were also observed in the actual condition to be carried by the pile cap. This means a more effective and efficient pile foundation design can be obtained by calculating the amount of load carried by both the pile and the pile cap, especially when the soil beneath the pile cap has sufficient stiffness.

The interaction between the soil and structure under workload can be reviewed to determine the load distribution in a foundation system. This is expected to be conducted through a full-scale field test using an optical fiber-optic instrument in order to determine the interaction between soil and structure along the pile and the pile cap.

1.1 Test Arrangement

Strain is normally measured using Distributed Fiber Optic Sensor Technology to investigate the pile-pile cap behavior during the axial static loading test. Foundation usually has a bored pile with a 1.6 m wide and 1.2 m high pile cap on top to carry the structural load.

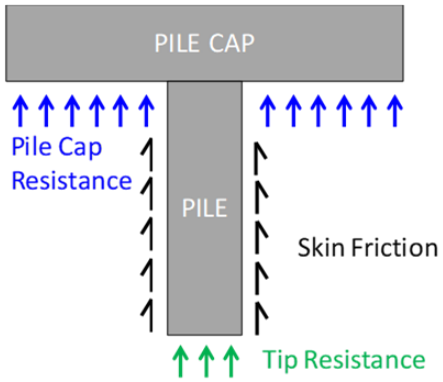

Figure 1 Bearing capacity contribution on Pile-Pile cap

The pile cap was installed on the top of the bored pile with 800 mm diameter and 2.7 m length and the pile-pile cap configuration is expected to provide an ultimate axial bearing capacity value of 190 tons×250%.

The measurement of the strain using the Distributed Fiber Optic Sensor Technology is required to derive the information regarding the pile-pile cap strain behavior at each loading step including the mobilized pile cap capacity, mobilized unit skin friction, and mobilized end bearing. Moreover, the fiber optic installed under the pile cap can be used to investigate the strain distribution in the soil, with a specific focus on a region.

2 MATERIALS AND METHOD

A static loading test was conducted on the bored pile (TP-02) to produce a compressive strength of 43.1 MPa while the concrete's modulus of elasticity, 30,820 MPa, was calculated using the compressive strength capacity of the concrete sample.

2.1 Piled – Raft Foundation

Piled-raft foundation is a combination of a pile and a raft foundation. A raft foundation with a larger bearing capacity is expected to have a more efficient dimension while the bearing and deformation behavior is characterized by the interaction between the bearing elements and the subsoil. Meanwhile, the interaction between the pile, raft, and soil is illustrated in Figure 2.

This means a total of four interactions are proposed and these include:

(i) Pile–soil interaction
(ii) Pile–pile interaction
(iii) Raft–soil interaction
(iv) Pile–raft interaction

Wiesner and Brown (1975) studied the effect of strip flexibility and pile stiffness on settlement and load carried by a pile and found that the load distribution and settlement on pile-raft are influenced by the stiffness of the pile and the raft. It was also discovered that the effect of the pile stiffness became more pronounced as the raft stiffness decreased. The solution produced by Wiesner and Brown based on the assumption of a long strip having 5 diameters with a single pile length of 50 diameters (L/d=50) is presented in Figure 3. Meanwhile, the pile stiffness factor (K) and strip flexibility factor (F_R) are the main determinants for the solutions as indicated in Equations (1) & (2).

$$K_p = \frac{E_p R_A}{E_s} \quad (1)$$

$$F_R = \frac{E_R I_R}{E_s D^4} \quad (2)$$

where:
K_p = pile stiffness
E_p = pile modulus
R_A = ratio of an area of pile section to the area bounded by pile outer-circumference
E_s = soil modulus
E_R = raft modulus
I_R = raft moment inertia
D = pile diameter

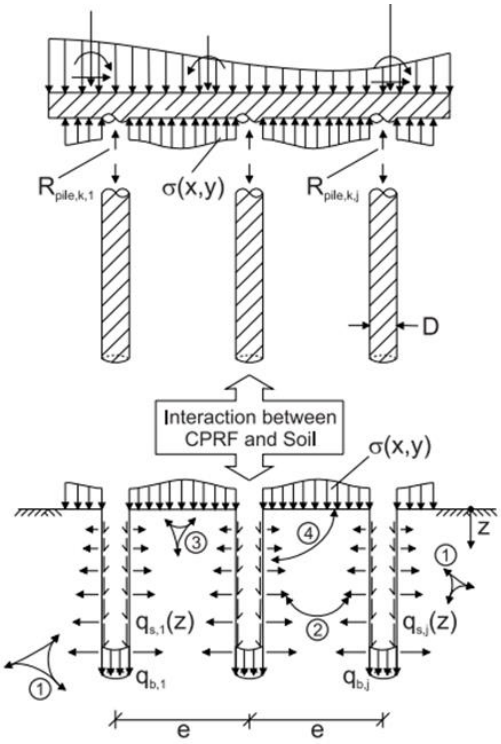

Figure 2 Soil and Pile Raft Interaction (Katzenbach, et al., 1998)

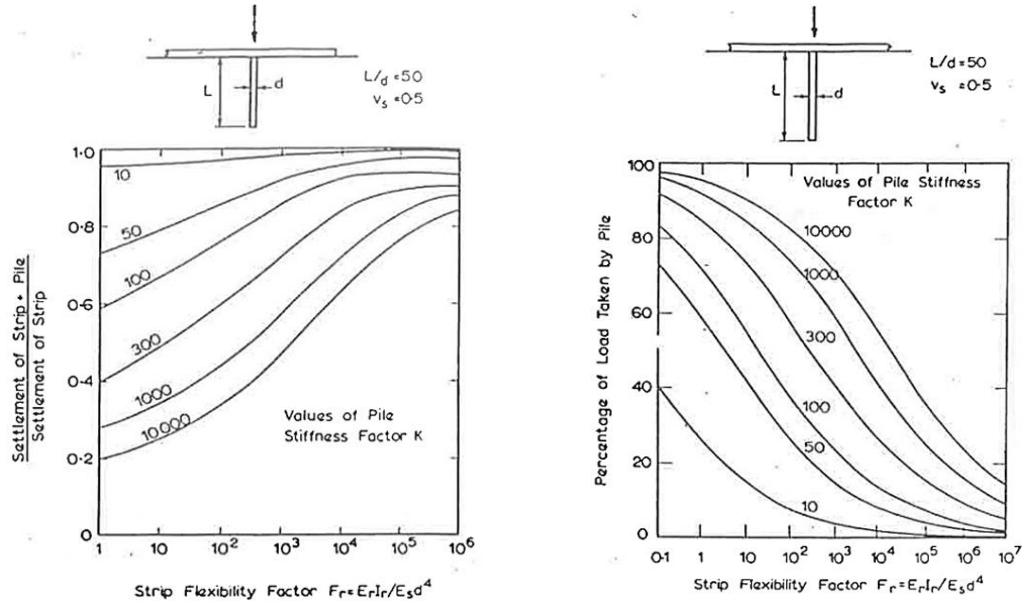

(a) (b)

Figure 3 (a) Effect of strip flexibility and pile stiffness on settlement (b) Effect of strip flexibility and pile stiffness on the load carried by the pile (Wiesner and Brown, 1975)

2.2 Bearing Capacity of Shallow Foundation

The ultimate bearing capacity when a foundation is supported by a weaker soil layer underlain by a stronger layer () can be given by empirical equation (Mayerhof, 1978; Hanna & Mayerhof, 1980):

$$q_u = q_t + (q_b - q_t)\left(1 - \frac{H}{D}\right)^2 \geq q_t \quad (3)$$

$$q_t = c_1 N_{c(1)} F_{cs(1)} + \gamma_1 D_f N_{q(1)} F_{qs(1)} + \frac{1}{2}\gamma_1 B N_{\gamma(1)} F_{\gamma(1)} \quad (4)$$

$$q_b = c_2 N_{c(2)} F_{cs(2)} + \gamma_2 D_f N_{q(2)} F_{qs(2)} + \frac{1}{2}\gamma_2 N_{\gamma(2)} F_{\gamma(2)} \quad (5)$$

where:

q_u = ultimate unit bearing capacity
q_t = ultimate unit bearing capacity upper layer
q_b = ultimate unit bearing capacity lower layer
D = depth of failure surface beneath the foundation (D ≈ B for loose sand and clay and D ≈ 2B for dense sand; Hanna & Mayerhof, 1980)
c' = effective cohesion of the soil
ϕ' = effective friction angle of soil
γ = unit weight of soil
q = overburden pressure
N_c, N_q, N_γ = bearing capacity factor
$F_{cs}, F_{qs}, F_{\gamma s}$ = shape factor

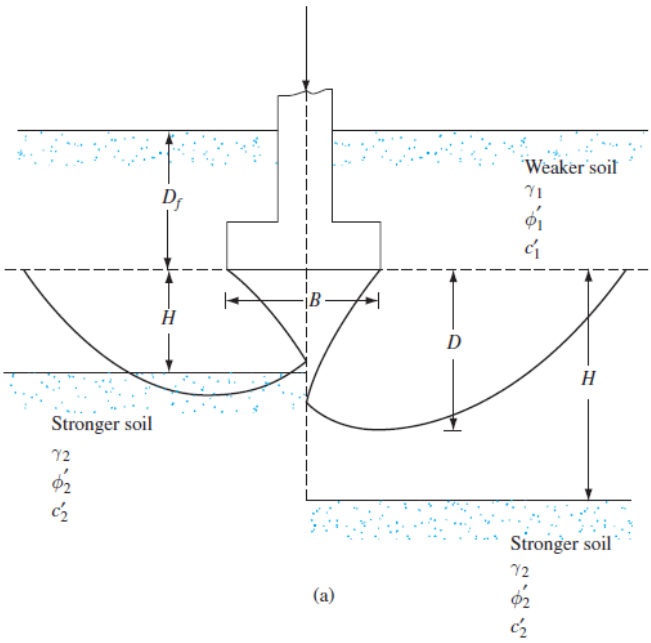

Figure 4 Foundation on weaker soil layer underlain by stronger soil layer (Das, 2011)

For clay soils with $\phi_1 = \phi_2 = 0$ then equations (4) and (5) are simplified to be as in equations (6) and (7).

$$q_t = \left[1 + 0.2\left(\frac{B}{L}\right)\right] c_{u(1)} N_c + \gamma_1 D_f \quad (6)$$

$$q_b = \left[1 + 0.2\left(\frac{B}{L}\right)\right] c_{u(2)} N_c + \gamma_2 D_f \quad (7)$$

2.3 Bearing Capacity of Bored Pile

The ultimate load-bearing capacity of a drilled shaft:

$$Qu = Qp + Qs \quad (8)$$

where:
Qu = ultimate capacity
Qp = ultimate load-carrying capacity at the base
Qs = skin resistance

2.3.1 Tip Resistance

The value of shear resistance at the tip of the pile for cohesive soils can be assumed to be $9 \times C_u$ (C_u = undrained shear strength) while Reese gives a correlation between the ultimate base resistance and NSPT value for cohesionless soils as indicated in Figure 5. The bearing capacity of the bored pile was calculated using an empirical method proposed by Reese and Wright (1977).

2.3.2 Shaft Resistance

The skin friction at the pile shaft was influenced by the type of soil and its strength. For cohesive soils, it can be defined as:

$$fs = \alpha \cdot cu \quad (9)$$

where:
α = adhesion factor
c_u = cohesion of undrained shear strength

The adhesion factor for bored piles in cohesive soil can be determined using the Kulhawy chart as shown in Figure 6. Meanwhile, the unit skin friction for the cohesionless soils was obtained from the correlation by Wright (1977) as shown in Figure 7.

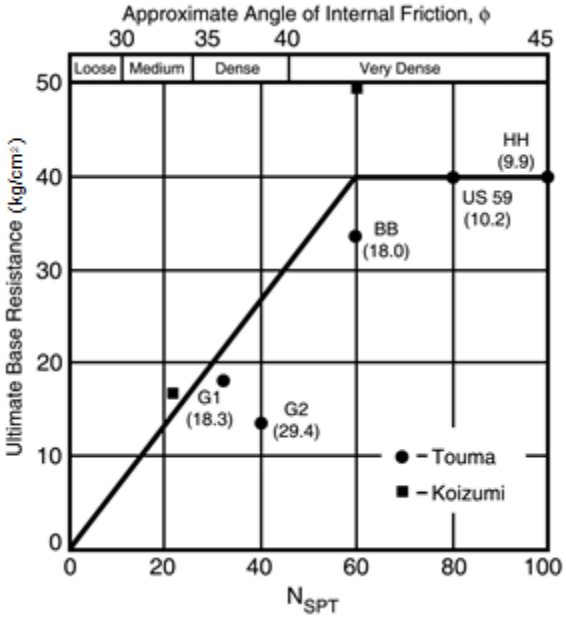

Figure 5 NSPT value vs. ultimate base resistance for cohesionless soils (Reese & Wright, 1977)

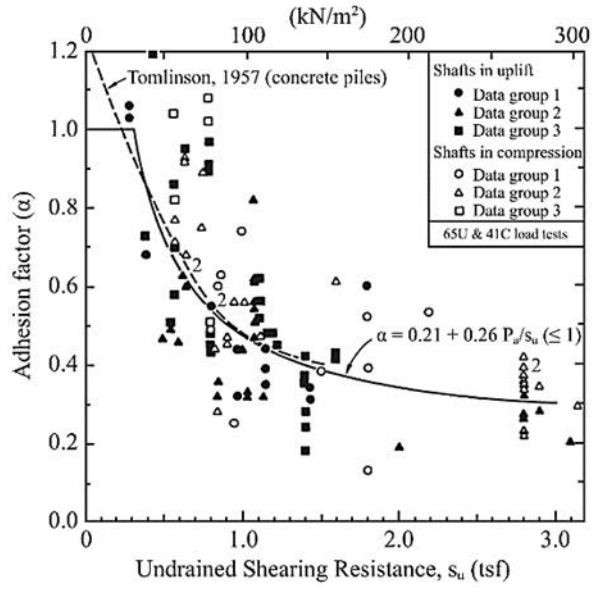

Figure 6 Adhesion factor vs. undrained shear strength (Kulhawy, 1991)

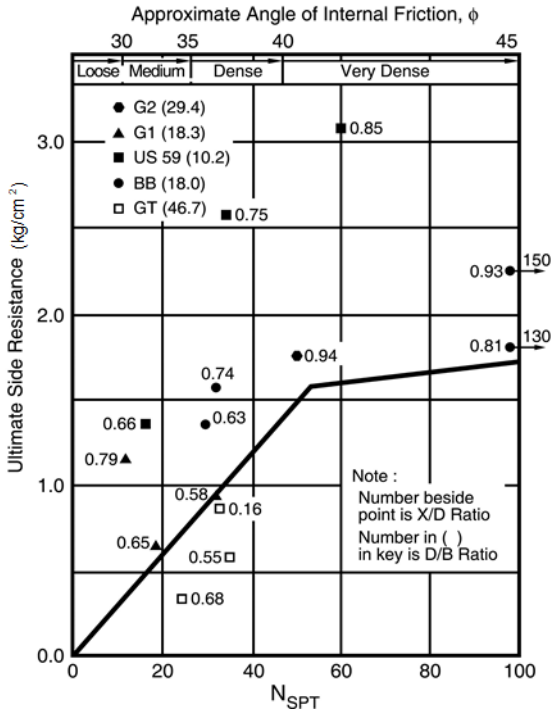

Figure 7 NSPT value vs. skin friction at shaft for cohesionless soils (Reese & Wright, 1977)

2.4 Distributed Fiber Optic Sensor Technology

The Distributed Fiber Optic Sensor Technology used to measure the strain behavior of the pile-pile cap was based on Brillouin Optical Time Domain Analysis (BOTDA) (George A S, 2016; Hisham & Tee, 2015). The system used two light sources which include the continuous and pulse waves from 2 sides of the fiber optic cable. The configuration of this light source produced stimulated Brillouin scattering (SBS) which when reflected was used to determine the Brillouin frequency of the fiber optic cable.

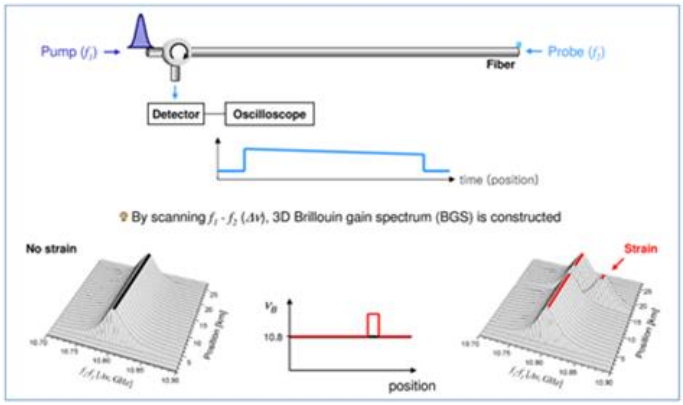

Figure 8 Principal Measurement of BOTDA system.

The Brillouin frequency shifted in the single-mode fiber is proportional to the change in the strain or temperature of the scattering location. The resolution of these frequency shifts and propagation time can be used to obtain a full strain profile. A particular advantage of BOTDA over other types of distributed strain sensing systems such as BOTDR (Brillouin Optical Time Domain Reflectometry) is that it produces a strong signal which has the ability to reduce the averaging times (faster acquisition time) and produce longer distance measurement capabilities (for up to 50 km). Moreover, every shift in the Brillouin frequency provides information on the changes in strain for every 40 mm fiber optic cable.

2.4.1 Test Preparation

The pile was installed using the common method in Indonesia while the pile cap was also constructed because the purpose of the test was to determine the behavior of the pile-pile cap. Moreover, the fiber optic was installed at the rebar (pile and pile cap) and right under the pile cap adjacent to the soil while the location of the pile is indicated in Figure 9.

A load cell and four dial gauges were also installed to measure the actual load transferred to the foundation and the pile top movement during the static loading test.

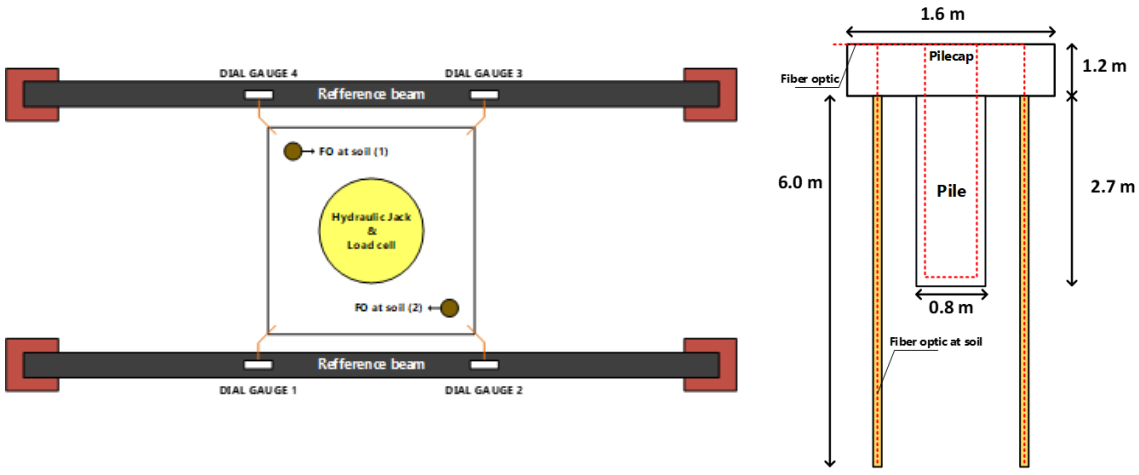

(a) (b)

Figure 9 (a) Instrumentation Configuration, (b) Fiber Optic Cable Location

Figure 10 Fiber Optic Installation

2.4.2 Soil Condition

The soil investigation data showed that TP-02 was embedded in the hard soil layer with an N_{SPT} value over 50. Meanwhile, the test pile elevation was at the cut area which is approximately 4 meters from the top of the test pile. The pile cap capacity was expected to contribute to the total bearing capacity at N_{SPT} 11 while the Cone Penetration Test (CPT) was conducted and a cone resistance lower than the value predicted from N_{SPT} was reported probably due to rainwater infiltration.

Subsurface condition can be described as follows:

1. Layer 1: Clayey silt with medium to firm consistency with N_{SPT} range 6 to 11 and q_c = 10 – 25 kg/cm^2 (0 – 5 m).
2. Layer 2: Hard silt with some gravel $N_{SPT} \geq 50$ (5 – 9 m) with CPT refused at depth 5.8 m.
3. Layer 3: Cemented silt with hard consistency $N_{SPT} \geq 50$ (9 – 14 m).
4. Layer 4: Clayshale with hard consistency $N_{SPT} \geq 50$ (14 – 30 m)

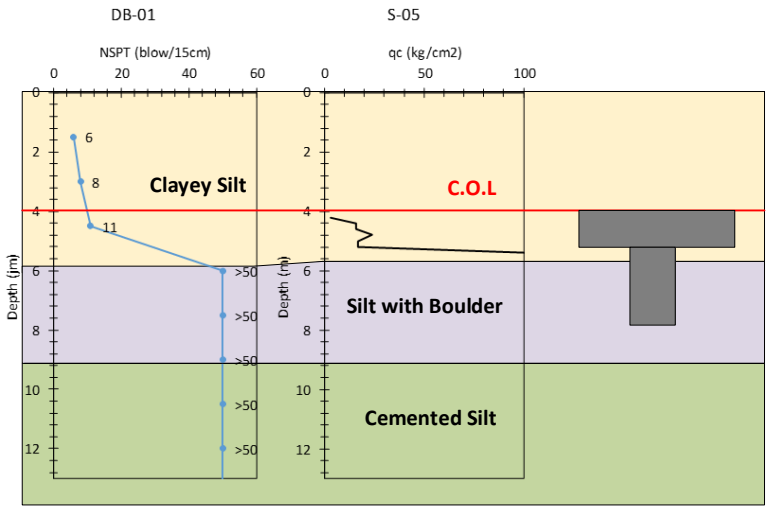

Figure 11 Soil Investigation Data

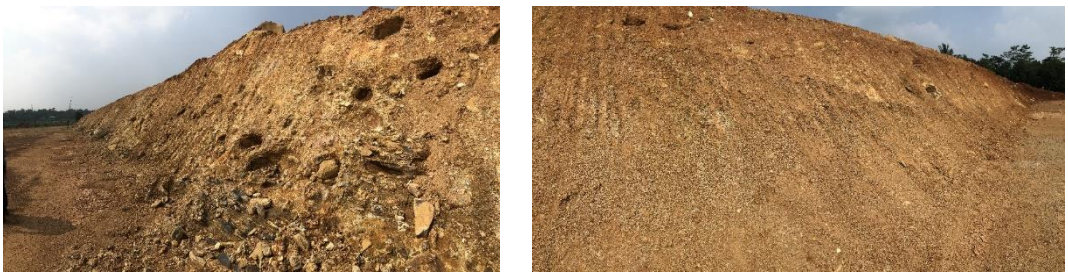

Figure 12 Field Condition

2.4.3 Calculation

The bearing capacity was calculated from both the pile cap and pile.

- Pile cap bearing capacity

  Pile cap rested on soil at N_{SPT} = 11 with the assumption shear strength 4 N_{SPT} therefore, the pile cap ultimate bearing capacity was calculated as follow:

  $\phi = 0^{\circ} \rightarrow N_c = 5.14$
  $D \approx B = 1.6$ m
  $D_f = 1{,}2$ m
  Upper layer → $c_{u(1)} = 4 \times 11 = 44$ kPa ; $\gamma_1 = 16$ kPa
  Lower layer → $c_{u(2)} = 50 \times 11 = 200$ kPa ; $\gamma_2 = 17$ kPa

  $$q_t = \left[1 + 0.2\left(\frac{B}{L}\right)\right] c_{u(1)} N_c + \gamma_1 D_f$$
  $$q_t = \left[1 + 0.2\left(\frac{1.2}{1.2}\right)\right] 44 \times 5.14 + 16 \times 1.2$$
  $$q_t = 290 \text{ kPa}$$

  $$q_b = \left[1 + 0.2\left(\frac{B}{L}\right)\right] c_{u(2)} N_c + \gamma_2 D_f$$
  $$q_b = \left[1 + 0.2\left(\frac{2}{2}\right)\right] 200 \times 5.14 + 17 \times 1.2$$
  $$q_b = 1254 \text{ kPa}$$

  $$q_u = q_t + (q_b - q_t)\left(1 - \frac{H}{D}\right)^2 \geq q_t$$
  $$q_u = 290 + (1254 - 290)\left(1 - \frac{0{,}8}{1.6}\right)^2$$
  $$q_u = 531 \text{ kPa} \approx 53 \text{ ton/m}^2$$

  $$Q_u = q_u A$$
  $$Q_u = 53 \times \left(1.6 \times 1.6 - \frac{1}{4}\pi(0.8)^2\right)$$
  $$Q_u = 109 \text{ ton}$$

- Soil bearing capacity of bored pile

  Shaft resistance was calculated using Kulhawy and Wright chart while the tip resistance was determined using the Wright chart. Therefore, the ultimate bearing capacity was calculated from the charts as follows.

  $$Q_s = f_s (\pi DL) = (4 \times 0.8\pi \times 0.2) + (17.7 \times 0.8\pi \times 0.2) = 113 \text{ ton}$$

  $$Q_p = q_p A = 400 \times \frac{1}{4}\pi(0.8)^2 = 200 \text{ ton}$$

  $$Q_u = Q_p + Q_s = 200 + 113 = 313 \text{ ton}$$

- Cumulative ultimate bearing capacity

  The ultimate bearing capacity for the pile-pile cap system can be determined using the cumulation of pile cap and bored pile bearing capacities but the result may not be accurate due to the existence of soil-structure interaction in the process.

  $$Q_{cum} = Q_{pile\ cap} + Q_{pile} = 109 + 313 = 422 \text{ ton}$$

Wiesner and Brown proposed the possibility of calculating the percentage of load carried by the pile and ratio settlement of strip + pile and settlement of strip. The pile stiffness factor (K) and strip flexibility factor (F_R) were calculated using the pile cap with 1.6 meters width and 1.2 meters height sitting on top of a bored pile with 800 mm diameter as follows:

$$K_p = \frac{E_p\, R_A}{E_s} = \frac{30820000 \times \frac{1.6^2}{0.25\pi\, 0.8^2}}{250000} = 630 \quad (10)$$

$$F_R = \frac{E_R\, I_R}{E_s\, D^4} = \frac{30820000 \times \frac{1}{12} \times 1.6 \times 1^3}{250000 \times 0.8^4} = 165 \quad (11)$$

The charts in Figure 3 showed the ratio of settlement of strip + pile and settlement of strip is 0.45 while the percentage of load carried by the pile was 73%. It is important to note that this value is not accurate because the chart was developed based on the assumption that L/d is 50 and the soil layer is uniform.

2.5 Load Test Procedure and Measurement

The Kentledge system was applied to conduct the axial static loading test on TP-02 and this involved using concrete blocks for the reaction load. Moreover, the preparation work and loading procedure were based on ASTM Standard D-1143.

(a) (b)

(c) (d)

Figure 13 Kentledge preparation work: (a) Compaction of subgrade soil, (b) Steel plate placing, (c) Installation of kentledge footing, main beam, secondary beam, and concrete block, (d) Kentledge system during pile test.

The preparation works started with soil bearing capacity investigation to ensure the capacity is sufficient to sustain the concrete block force. Moreover, the subgrade bearing capacity was required to be tested to ensure soil condition is consistent while a steel plate was used to distribute the load from the kentledge footing. A high-capacity steel frame was also placed at the footing of the kentledge system followed by the main beam which was connected to the secondary beam holding the concrete block.

3 RESULTS

3.1 Loading Test Result

The loading schedule consists of five cycles to achieve 250% of the design load. Meanwhile, one of the dial gauges almost reached its limit at 190% and this led to a stop in the progressive load increment while the current load was held up to the moment the settlement rate was under 0.25 mm/hour. The loading steps and the duration are presented in Figure 14.

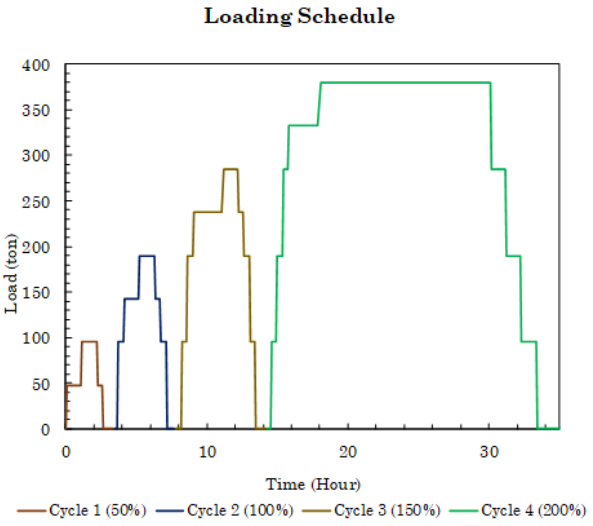

Figure 14 Loading step and duration on TP-02

Figure 15 shows that the top settlement in cycles three and four increased significantly. It is important to note from the soil test that the foundation system is embedded at a hard soil layer with an N_{SPT} value over 50 but the settlement increased significantly when loaded. This was associated with the existence of mud at the bottom of the pile.

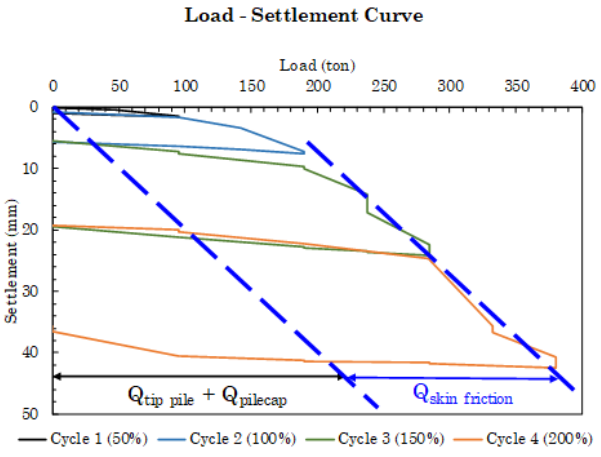

Figure 15 Load – settlement curve TP-02

An alternative method of interpretation using the load – settlement curve was based on the concept that the load was carried mostly by the skin resistance until the shaft slip was sufficient to mobilize the limiting value. Moreover, the point load increased when the limiting skin resistance was mobilized almost linearly until the ultimate point capacity was reached. At this point, further loads applied led to a direct settlement with the load curve becoming vertical. This concept was introduced by Van Weele (1957) and has since been used by several others.

Figure 15 shows that the ultimate shaft resistance was 170 tons as indicated in the blue line and tip resistance + pile cap bearing capacity was 220 tons as represented by the black line. The calculations made using this method were quite close to the results obtained from the measurements using optical fiber such as the skin friction based on the strain measurement recorded to be 202 tons. It is also important to note that the skin friction value of the bored pile from the measurement was higher than the value proposed by Reese and Wright (1977). This is possibly due to the fact that sandy soil interacts with cement to cause higher skin friction. Meanwhile, Reese and Wright chart ultimate shaft resistance is only limited to 1.75 kg/cm^2.

3.2 Fiber Optic Result

This research used two fiber optics to measure strains with one placed in the rebar which is the bored pile and pile cap and another under the pile cap to measure the soil strain beneath the cap. The values were recorded up to 150% of the design load due to an electronic problem at the last cycle.

3.3 Load Carried by the Pile cap

The load carried by the pile cap and its percentage are shown in Figure 12 and it was discovered that an increase in the load led to an increment in the pile cap's resistance. However, the load carried by the pile cap showed a constant value of ± 14 tons at 75% – 125% design load (142.5 – 237.5 tons) while a relatively high increase in the carrying capacity of the pile cap with the value doubled to 30 tons was observed at cycle 150%.

3.4 Load Transfer

The load transferred along the pile was calculated based on strain and the concrete's modulus of elasticity which was assumed to be 30820 MPa.

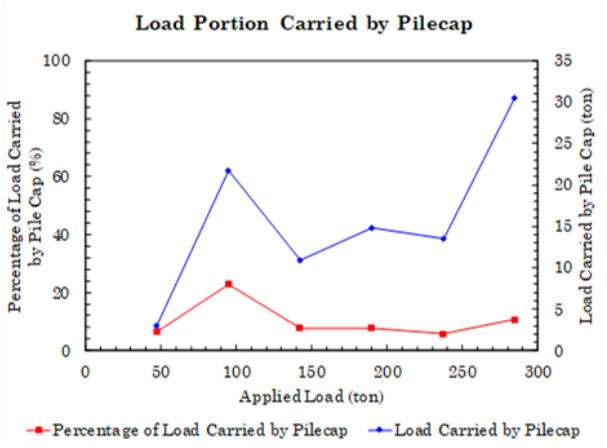

Figure 16 Load portion carried by the pile cap

The load transfer for each cycle presented in Figure 17 shows that skin friction is more dominant than the tip resistance even though the pile was embedded in the hard soil layer. According to Reese and Wright chart with an N_{SPT} value >50, the ultimate base resistance was able to reach 40 kg/cm^2 while the strain measurement showed that the mobilized unit end bearing was 8.5 kg/cm^2. This is possibly due to the existence of some mud at the bottom of the pile cap.

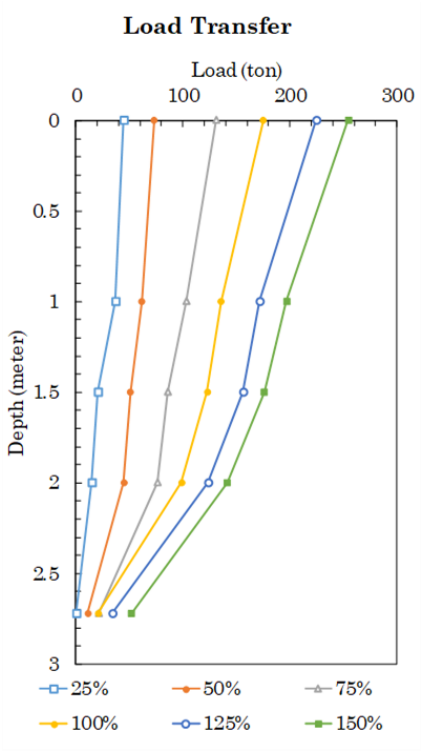

Figure 17 Load transfer of tested pile

The mobilized unit end bearing was 854 kPa with 18.2% of the total load being carried at the top of the pile during 150% of the design load. The remaining 81.8% was carried by the pile skin friction and pile cap resistance. Wiesner and Brown's chart also showed that the percentage of load carried by the pile was 45% and this means the values are not compatible.

3.5 Mobilized Unit Skin Friction and Mobilized End Bearing

It is possible to calculate the shortening at each point along the pile. The process involves integrating the change of strain profile from top to bottom in order to obtain an estimation of the internal displacement of each point along the pile, relative to the top. This cumulative pile shortening from the top of the pile cap for each cycle is shown in Figure 18 and the maximum was recorded to be 0,24 mm. This relatively small value is probably due to the short length of the pile (±2.7 m). Moreover, this means the settlement at the top of the pile cap is relatively the same as the settlement at the pile toe but this is not compatible with Wiesner and Brown chart.

The mobilized unit skin friction and mobilized end bearing were calculated based on load transfer analysis. This is observed from the summary of the skin friction mobilized at each loading stage in the segment reviewed based on the results of the mobilization along the pile segment in Table 1.

Table 1 Mobilized unit skin friction

Depth (m)	Unit Skin Friction (kPa) at Applied Load (%)					
	25	50	75	100	125	150
0.0 – 0.5	29	42	104	143	190	210
0.5 – 1.0	114	79	120	95	112	147
1.0 – 1.5	41	43	69	172	232	251
2.0 – 2.7	76	169	276	392	452	449

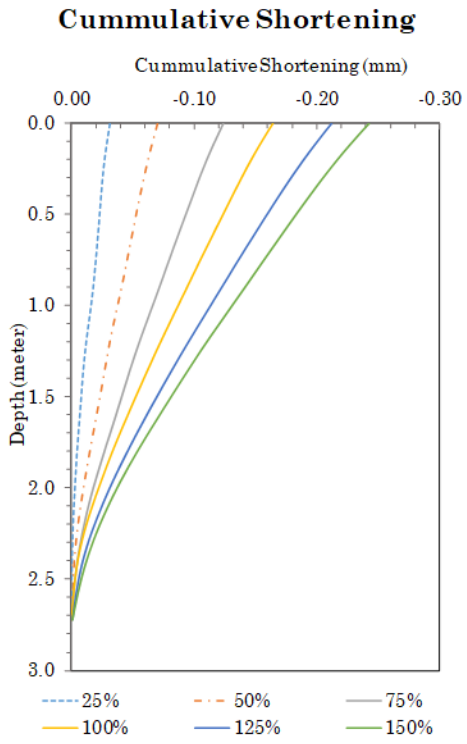

Figure 18 Cumulative shortening of tested pile

The mobilized unit skin friction from 0 to 1.5 meters was estimated to be 29 kPa to 251 kPa while higher unit skin friction was found at 1.5 to 2.7 meters in depth. It is important to note that the value from the measurement is higher than the one proposed by Reese and Wright (1977) and this is possibly due to the fact that sandy soil interacts with cement.

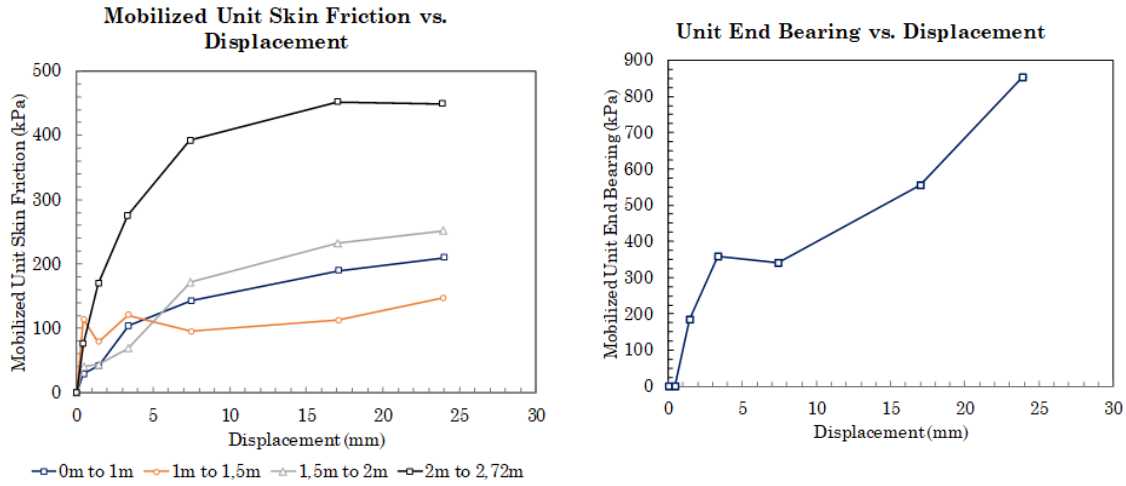

(a) (b)

Figure 19 The graphs of (a) τ-z curve, (b) q-z curve

These data can be used to develop τ-z (unit skin friction vs. displacement) and q-z curve (unit end bearing vs. displacement) but the q-z was not developed fully because the results recorded are only up to 150% of the design load.

3.6 Strain In the Soil Below the Pile Cap

The fiber optic was installed in soil under the pile cap and was expected to record strain in soil during the axial loading. The installation was made on the left and right sides which is 6 meters long as indicated in Figure 9B. The strain was measured for each cycle and the result is presented in Figure 20.

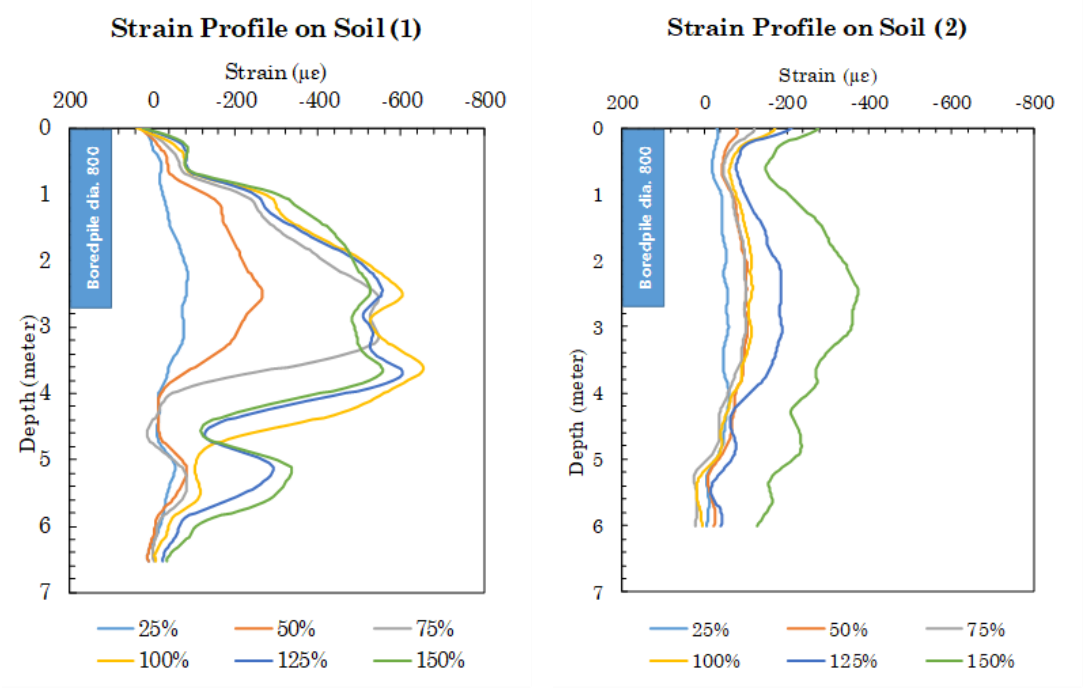

(a) (b)

Figure 20 The results of strain measurements due to the axial loading (a) left side, (b) right side

The strain measurements on the soil made the zone of influence due to the loading of the foundation to reach two times the length of the pile while the biggest zone of influence lies at the end of the foundation. A greater strain was also measured from depth 0 – 4 meters and this means the layer is softer than the layer beneath. Moreover, the strain on the left side (1) showed a higher value than on the right side (2) and this is probably due to the eccentricity of the load.

4 DISCUSSION

This study aims to understand the pile-pile cap interaction during loading but the measurement was recorded up to 150% of the design load due to an electronic problem at the last cycle.

The strain measurement showed that the pile cap's portion of the load was approximately 6% to 23% from the actual load applied at the top. It was also discovered that the load carried by the pile cap shows a constant value of ± 14 tons at cycle 75% to 125% of the design load (142.5 – 237.5 tons) and this is relatively low. However, the increase in the carrying capacity of the pile cap was relatively high with 30 tons at cycle 150% of the design load.

The mobilized unit skin friction from 0 to 1.5 meters was estimated to be 29 kPa to 251 kPa while higher unit skin friction was found at 1.5 to 2.7 meters in depth. It is important to note that the value from the measurement is higher than the one proposed by Reese and Wright (1977) and this is possibly due to the fact that sandy soil interacts with cement. Meanwhile, Reese and Wright chart ultimate shaft resistance is only limited to 1.75 kg/cm^2.

The concept that has the ability to determine shaft resistance and tip resistance based on the load – settlement curve which was introduced by Van Weele (1957) was also applied and the ultimate shaft

resistance was found to be 170 tons while the tip resistance + pile cap bearing capacity was 220 tons. This means the results obtained from this method are quite close to the values from the measurements made using the optical fiber. This is observed from the 202 tons recorded for the skin friction based on the strain measurement.

The mobilized unit end bearing was recorded to be 854 kPa with 18.3% of the total load carried at the top of the pile during 150% of the design load while the remaining 81.7% was carried by the pile skin friction and pile cap resistance. Moreover, the end-bearing result obtained from the measurement is relatively low even though the pile was embedded in the hard soil layer. According to Reese and Wright chart with an NSPT value >50, the ultimate base resistance is 40 kg/cm^2 while the strain measurement showed that the mobilized unit end bearing was 8.5 kg/cm^2. This is probably due to the existence of some mud at the bottom of the pile.

According to Wiesner and Brown's chart, the ratio of the settlement of strip + pile and settlement of strip is 0.45 while the percentage of load carried by the pile is 73%. These values are not compatible with the result obtained from the strain measurement and this means the chart cannot be applied to this case because it assumes that L/d = 50 with a uniform soil layer.

The strain measurements on the soil also showed that the zone of influence due to the loading of the foundation reaches two times the length of the pile while the biggest zone of influence lies at the end of the foundation. This is a visible indication of a load eccentricity between the left and right sides of the pile cap.

5 CONCLUSIONS

The fiber optic instrumentation demonstrated that the system is capable of measuring the pile and pile cap load capacities.

The load portion carried out by pile cap was approximated at 6% to 23% from the actual top load applied. Moreover, the load carried by the pile cap shows a constant value of ± 14 tons at cycle 75% to 125% of the design load (142.5 – 237.5 tons) and this is relatively low. However, the increase in the carrying capacity of the pile cap was relatively high with 30 tons at cycle 150% of the design load.

The skin friction obtained from the Van Weele method (170 tons) is similar to the strain measurements (202 tons) but quite different from the calculation (113 tons). Furthermore, the skin friction of the bored pile from the measurement is higher than the value proposed by Reese and Wright (1977) and this is probably because sandy soil interacts with cement, thereby, leading to higher skin friction. It was also discovered that the ultimate shaft resistance in Reese and Wright chart is only limited to 1.75 kg/cm$^{2.}$

Wiesner and Brown's chart cannot be applied to this case because it assumes that L/d = 50 with a uniform soil layer but it was able to provide a proportion of load carried by the pile and pile cap and, most importantly, the rigidity or flexibility factor.

The mobilized unit end bearing was calculated to be only 8.5 kg/cm^2 even though the pile was embedded in the hard soil layer while Reese and Wright's chart with NSPT value >50 showed the ultimate base resistance is 40 kg/cm^2. This is possible because of some mud existing at the bottom of the pile.

DISCLAIMER

The authors declare no conflict of interest.

AVAILABILITY OF DATA AND MATERIALS

All data are available from the author.

ACKNOWLEDGMENTS

The first author gratefully acknowledges the scholarship from Parahyangan Catholic University and immensely grateful to PT. Geotechnical Engineering Consultant (GEC) for provided data and greatly assisted the research.

REFERENCES

Das, B M., 2011. *Principles of Geotechnical Engineering 7th Edition.* USA.

George, A S., 2016. Distributed Fiber Optic Sensors-Brillouin Optical Time Domain Analysis (BOTDA) Sensor in Simple Language. *International Journal of Engineering Research,* 5(2), pp. 131-136.

Hanna, A. M., & Meyerhof, G G., 1980. Design Chart for Ultimate Bearing Capacity of Foundations on Sand Overlying Soft Clay. *Canadian Geotechnical Journal*, 17(2), https://doi.org/10.1139/t80-030

Kulhawy, F. H., 1991. Foundation engineering handbook: Drilled shaft foundations. Springer

Katzenbach, R., Arslan, U., Moormann C & Reul, O., 1998. Piled Raft Foundation: Interaction Between Piles and Raft. *Darmstadt Geotechnics*, 4(2), pp. 279-296.

Meyerhof, G G., 1974. Ultimate Bearing Capacity of Footings on Sand Layer Overlying Clay. *Canadian Geotechnical Journal*, 11(2), https://doi.org/10.1139/t74-018

Mohamad, Hisham, & Bun Pin Tee, 2015. Instrumented Pile Load Testing with Distributed Optical Fiber Strain Sensor. *Jurnal Teknologi*, 77(11).

Reese, L. C., & Wright, S. J.,1977. *Drilled Shaft Design and Construction Guidelines Manual (Vol. 1)*. Department of Transportation, Federal Highway Administration, Offices of Research and Development, Implementation Division.

Van Weele, A. F., 1957. A method of separating the bearing capacity of a test pile into skin friction and point resistance. *Proceedings of the Fourth International Conference on Soil Mechanics and Foundation Engineering*.

Wiesner, T.J. & Brown, P.T., 1975. Behavior of Piled Strip Footings Subjected to Concentrated Loads. *Civ. Eng. Res. Rep. R275. Univ of Sydney, Aus*.